

# APPLICATION OF A WAX DEPOSITION MODEL IN OIL PRODUCTION PIPELINES

## *APLICACIÓN DE UN MODELO DE DEPOSICIÓN DE PARAFINAS A TUBERÍAS DE PRODUCCIÓN DE CRUDOS*

Diego-Fernando Bautista-Parada<sup>1</sup>, David-Alfredo Fuentes-Díaz<sup>1</sup>, Paola Gauthier-Maradei<sup>2</sup>  
and Arlex Chaves-Guerrero<sup>1\*</sup>

<sup>1</sup>GIEMA, Escuela de Ingeniería Mecánica, Universidad Industrial de Santander, Bucaramanga, Santander, Colombia

<sup>2</sup>INTERFASE, Escuela de Ingeniería Química, Universidad Industrial de Santander, Bucaramanga, Santander, Colombia

e-mail: achavesg@uis.edu.co

(Received: Nov. 19, 2014; Accepted: Apr. 15, 2015)

### ABSTRACT

This work is aimed to study the wax deposition process on the internal surface of oil production pipelines and the influence of parameters such as flow rate and pipe wall temperature on the deposit thickness for a light crude oil with high paraffinic content considering three different temperature boundary conditions on the pipe wall; two of which assumed a profile temperature on the boundary, fact that has not been considered in previous works, and the third a constant value. The analysis was conducted assuming pseudo steady conditions on the fluid phase. The finite differences method was applied to solve the differential equation system and the solution was implemented numerically using the C++ programming language. The model was validated with the experimental results reported by Singh *et al.* (2000) and subsequently used to simulate the growth of the paraffin deposits as a function of flow rate and pipe temperature. The results showed that increased flow rates reduce the maximum deposit thickness, as it spreads on a longer distance in the pipe when considering a constant wall temperature or the axial thermal gradient with a positive slope, and the opposite effect is observed when considering the axial thermal gradient with a negative slope.

**Keywords:** Paraffin deposition models, Flow assurance, Paraffinic crude oils, CFD, Crude oil transportation.

**How to cite:** Bautista-Parada, D. F., Fuentes-Díaz, D. A., Gauthier-Maradei, P. & Chaves-Guerrero, A. (2015). Application of wax deposition model in oil production pipelines. *CT&F - Ciencia, Tecnología y Futuro*, 6(1), 29-42.

\*To whom correspondence should be addressed

## RESUMEN

---

**E**l objetivo de este trabajo es estudiar el proceso de deposición de parafinas sobre la superficie interna de las tuberías de producción de petróleo y la influencia de parámetros como la velocidad de flujo y la temperatura de la pared sobre el espesor del depósito para un crudo ligero con alto contenido parafínico considerando tres condiciones de frontera sobre la pared de la tubería; dos de las cuales suponen un perfil de temperatura en la frontera, hecho que no ha sido considerado en trabajos anteriores, y la tercera un valor constante. El análisis se realizó suponiendo condiciones seudo-estables en la fase fluida. El método de diferencias finitas se aplicó para resolver el sistema de ecuaciones diferenciales y la solución se llevó a cabo numéricamente utilizando el lenguaje de programación C++. El modelo fue validado a partir de los resultados experimentales reportados por Singh *et al.* (2000) y posteriormente utilizados para simular el crecimiento de los depósitos de parafina como una función de la velocidad de flujo y la temperatura de la tubería. Los resultados mostraron que el aumento de la velocidad de flujo reduce el máximo espesor del depósito, pero este se extiende sobre una distancia más larga sobre la tubería cuando se considera una temperatura de pared constante o cuando se considera el gradiente de temperatura axial con pendiente positiva; mientras que se observa el efecto contrario cuando se considera el gradiente de temperatura axial con pendiente negativa.

---

**Palabras clave:** Modelos de deposición de parafinas, Aseguramiento de flujo, Crudos Parafínicos, CFD, Transporte de crudos.

## RESUMO

---

**E**sse trabalho objetiva estudar o processo de deposição de parafinas sobre a superfície interna dos tubos de produção de petróleo e a influência de parâmetros como a velocidade de fluxo e a temperatura da parede sobre a espessura do depósito para um petróleo leve com alto conteúdo parafínico considerando três condições fronteira sobre a parede do tubo; sendo que dois delas pressupõem um perfil de temperatura na fronteira, fato que não foi considerado em trabalhos anteriores, e a terceira um valor constante. A análise foi feita com a presunção de condições pseudo-estáveis na fase fluida. O método de diferenças finitas foi aplicado para a resolução do sistema de equações diferenciais e a solução foi atingida de forma numérica utilizando a linguagem de programação C++. O modelo foi validado com base nos resultados experimentais relatados por Singh *et al.* (2000) e posteriormente utilizados para a simulação do crescimento dos depósitos de parafina como uma função da velocidade de fluxo e da temperatura do tubo. Os resultados demonstraram que o aumento da velocidade de fluxo reduz a espessura máxima do depósito, no entanto, ele se estende sobre uma distância maior sobre o tubo quando considerada a temperatura de parede constante ou o gradiente de temperatura axial com inclinação positiva; enquanto se verifica o efeito contrário quando considerado o gradiente de temperatura axial com inclinação negativa.

---

**Palavras-chave:** Modelos de deposição de parafina, Aseguramento do fluxo, Parafina cru, CFD, Transporte de petróleo cru.

## 1. INTRODUCTION

Paraffin deposition on the internal surface of pipelines is common during oil transportation under the sea, where temperatures are around 4°C. In this case, deposition is caused by low temperatures leading to a decreased solubility of the paraffin in the crude mixture. However, it has also been observed that some light crude oil with high paraffinic content produced on shore, undergoes a solubility decrease under less severe temperature conditions. This problem has caused huge economic losses to the petroleum industry due to progressive clogging of production lines, therefore it is mandatory to implement techniques to reduce or control this phenomenon. Thus, it is of the essence to properly validate models that can predict the behavior of the deposition phenomenon for each specific situation occurring within each production field; such as the geographical position of the field as well as the physical and chemical properties of the crude oil.

This work is aimed to study the paraffin deposition process and the influence of flow rate on the deposit thickness for a crude oil with high paraffinic content when applying three different temperature boundary conditions on the pipe surface, two of which consider a temperature profile, representing the offshore and onshore production situations; by implementing the model proposed by Singh *et al.* (2000) which has been only applied to a constant value of pipe wall temperature only under laboratory conditions. The finite volume method was applied to solve the differential equation system and the solution was implemented numerically by using the C++ programming language. The model was validated with the experimental results reported by Singh *et al.* (2000) and then used to simulate the deposit growing for a particular case using a sample of highly paraffinic oil from a Colombian oil field.

A paraffin deposition model is mainly purported to calculate the location and the growth rate of the paraffin layer in the internal wall of a production or transportation oil pipeline. For this purpose, a variety of theories considering molecular diffusion, shear dispersion, Brownian diffusion and gravity settling (Burger, Perkins & Striegler, 1981) have been raised. Furthermore, the phenomenological description needs to take into account the thermodynamic nature of the

problem and the moving boundary between the fluid-gel layer and the fluid phase.

There are models strictly based on thermodynamic concepts that allow for characterizing the equilibrium between oil and paraffins in order to predict the Wax Appearance Temperature (WAT) and the solubility curves of paraffin into the crude mixture (Coutinho & Daridon, 2001; Coutinho, Mirante & Pauly, 2006). However, these models can not predict the growth rate of the paraffin deposit and its location in the pipeline.

Other models consider the hydrodynamic effect and energy and mass transport, typical of the phenomenon; the disadvantage of these models is that the solution requires a simultaneous solution of the equations of mass and energy conservation in the solid and liquid phases and at their interface; which brings about a greater difficulty. Svendsen (1993) was perhaps the first author who introduced a mathematical model to quantify and predict the deposited wax in a horizontal pipe. This model uses simplified correlations to predict the velocity field and the temperature profile, however the main failure occurs as result of assuming a constant value of wax content into the paraffin layer; since, experiments have shown significant variations regarding wax content in the axial and radial directions (Singh *et al.*, 2000).

After Svendsen (1993), other models have been presented, such as the RRR (Rygg, Rydahl and Rønningsen, 1998) model developed by the Tulsa University (Matzain *et al.*, 2001) and the model proposed by the Michigan University (Singh *et al.*, 2000). On the one hand, RRR is a multiphase flow model that predicts paraffin deposition in production wells when exclusively operated in turbulent regime (Hoveden *et al.*, 2004). Matzain *et al.* (2001) is a semi-empirical kinetic model that predicts the thickness of paraffin deposits with an acceptable accuracy, especially when using high flow rates. This model and the RRR model consider the molecular diffusion and shear dispersion as the mechanisms that cause deposition (Gjermundsen, 2006).

On the other hand, the Michigan University model (Singh *et al.*, 2000) can be applied for a single-phase flow either under laminar or turbulent regimes. This

is the only model that considers the paraffin fraction change into the deposit and does not require adjustable parameters that could hinder the implementation; even more importantly, it is necessary to know the physical properties of oil and the system operating conditions, which all in all renders this model the most suitable for implementation.

This study used the model proposed by Singh *et al.* (2000) which has been validated experimentally and recently improved by Huang *et al.* (2011) and Lu *et al.* (2012). In their model, they consider mass diffusion as the only transport mechanism for paraffins, therefore accounting for the build-up of pipeline deposits when considering a laminar flow regime.

## 2. THEORETICAL FRAMEWORK

### Deposition Mechanism

The mechanism described below was proposed by Singh *et al.* (2000), experimentally validated and accepted by different authors, including Lee (2007). This mechanism assumes that when a mixture of paraffinic crude get in touch with a surface with a lower temperature than crude; the nearest fluid layer to the wall loses heat and temperature decreases rapidly reaching the limit of solubility of the crude mixture and starts growing an incipient gel layer over the cold surface.

When considering a cylindrical geometry as the one found in production pipes, the temperature difference between the fluid and the wall generates a temperature gradient in radial direction; which causes a concentration gradient in the same direction due to the dependence of the wax solubility on the temperature, while allowing for the mass transport through the fluid-gel interface. Once paraffin is transported to the interface, a diffusion process through the gel layer takes place, increasing wax concentration in the deposit. Nevertheless, paraffins are not completely transported to the deposit; one part of these accumulates in the interface, which enables the deposit to grow, as shown in Figure 1.

### Deposition Model

The phenomenological formulation of paraffin deposition in pipes must take into account the thermodynamic nature of the problem and the moving boundary established between the gel layer (deposit)

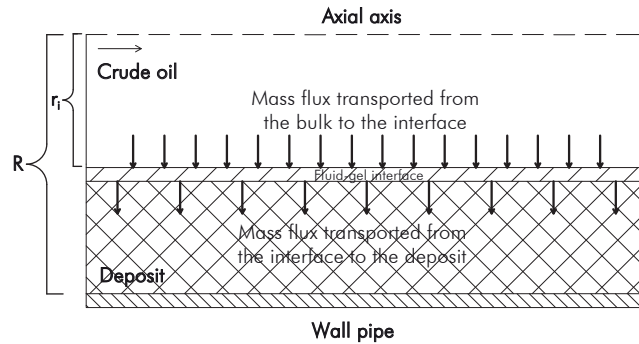


Figure 1. Deposition mechanism proposed by Singh *et al.* (2000). In this case,  $R$  is the inner pipe radius and  $r_i$  is the deposit position.

and the crude (fluid). In order to solve this problem it is necessary to put forward a mass and energy balance regarding fluids and deposits. In case of fluids, energy (Equation 1) and mass (Equation 2) balances have been proposed, assuming diffusion in radial coordinate and convection in axial direction.

$$v_z \frac{\partial T}{\partial z} = \frac{1}{r} \frac{\partial}{\partial r} \left( r \alpha_r \frac{\partial T}{\partial r} \right) \quad (1)$$

$$v_z \frac{\partial C}{\partial z} = \frac{1}{r} \frac{\partial}{\partial r} \left( r D_{wo} \frac{\partial C}{\partial r} \right) \quad (2)$$

Where,  $\alpha_r$  is the thermal diffusivity and  $D_{wo}$  is the paraffin diffusivity in the oil. The boundary conditions for mass and energy balances in the fluid are shown in Table 1.

Table 1. Boundary conditions for mass and energy balances in the fluid.

Coordinate	Energy	Mass
$r=r, z=0$	$T=T_{in}$	$C=C_{in}$
$r=0, z=z$	$\frac{\partial T}{\partial r}=0$	$\frac{\partial C}{\partial r}=0$
$r=r_i, z=0$	$T=T_w$	$C=C_{ws}(T)$

Analysis of the paraffin deposit takes molecular diffusion as the dominant mechanism of wax diffusion inside the deposit; therefore, mass transport within the deposit contributes to increasing the wax fraction and the deposit thickness. To determine the flux transported from the pipe middle section to the wall one assumes that the convective transport in the deposit is negligible and that the diffusive transport of wax can be approximated by the diffusive transport of wax in the fluid phase evaluated on the interface (Equation 3).

$$\pi\rho_{gel}(R^2 - r_i^2)L \frac{dF_w}{dt} = 2\pi r_i L \left( -D_e \frac{dC_{ws}}{dr} \Big|_{r_i} \right) \quad (3)$$

In Equation 3,  $R$  is the inner pipe radius,  $r$  is the radial coordinate,  $r_i$  is the interface position,  $F_w$  is the mass fraction of the gel,  $L$  is the length of the pipe,  $\rho_{gel}$  is the wax density,  $C_{ws}$  is the paraffin solubility in the oil and  $D_e$  is the effective diffusivity in the deposit as given by Cussler *et al.* (1998) (Equation 4).

$$D_e = \frac{D_{wo}}{1 + \alpha^2 F_w^2 / (1 - F_w)} \quad (4)$$

Where,  $\alpha$  is the aspect ratio of the wax crystals in the deposit,  $D_{wo}$  is the molecular diffusivity of wax in oil and was given by Hayduk and Minhas (1982).

$$D_{wo} = 13.3 \times 10^{-8} \left( \frac{T^{1.47} \mu^\gamma}{V_A^{0.71}} \right) \quad (5)$$

$$\gamma \equiv \frac{10.2}{V_A} - 0.791 \quad (6)$$

In Equation 5,  $T$  is absolute temperature,  $\mu$  is solvent viscosity and  $V_A$  is the wax molar volume, while in Equation 6,  $\gamma$  is a function of  $V_A$ .

Regarding the interface, Singh *et al.* (2000) proposed an interfacial balance of wax, which is shown in Equation 7:

$$2\pi r_i F_w(t) \rho_{gel} \frac{dr_i}{dt} = 2\pi r_i F_i [C_{ws}(T_i)] - 2\pi r_i \left( -D_e \frac{dC_{ws}}{dr} \Big|_{r_i} \right) \quad (7)$$

Where,  $k_i$  is the mass transfer coefficient and  $C_{wb}$  is the bulk concentration of wax molecules. Equation 7 implies that the growth speed of the deposit is determined by the difference between the wax flux normal to the interface in the deposit and the fluid phase, evaluated at the interface.

### Assumptions

This model applies for pipelines presumably working under pseudo steady conditions and neglecting any thermal energy generation in the fluid. The fluid is assumed to be Newtonian and incompressible while density of paraffin is assumed to be equal to the oil. The WAT depends on the maximum amount of wax dissolved in solution. Above the WAT, the flow is

deemed a single-component and also a binary mixture of oil and paraffin. This analysis assumes that the oil is free of water and gas. Pipe wall temperature was assumed to be constant in the case used for validation and variable in the two remaining cases. The solid paraffin content in the deposit is assumed to increase with time. Additionally, the model only considers the molecular transport of mass and heat in the radial direction in the deposit and in the fluid phase while the convective transport is only considered in the axial direction in the fluid phase. In relation to these assumptions, Tian *et al.* (2014) conducted a study to verify the effect of dropping the axial heat conduction term in the energy balance of the deposit by comparing the temperature profiles obtained from a unidirectional model versus the one obtained considering heat conduction in axial and radial directions. To this end, Tian *et al.* (2014) used the temperature profile obtained by Svendsen (1993) for the fluid phase in order to find the boundary condition in the fluid-deposit interface for three fixed values of deposit thickness (without calculating the deposit thickness) avoiding to resolve simultaneously the mass and energy balances at the deposit-fluid interface. Finally, Tian *et al.* (2014) confirm that neglecting the term heat conduction in the axial direction in the energy balance is feasible. Another important assumption taken into account in this model, is that the paraffin deposit is so thin that the flow field is well represented by vector  $\mathbf{v} = v_z(r) \mathbf{i}_z$ , omitting the radial component of velocity generated by the cross-sectional pipe reduction associated to the deposit growth and by the mass diffusion at the radial direction. This assumption may result in an underestimation of the deposit size.

## 3. MODEL NUMERICAL IMPLEMENTATION

### Solution Algorithm

The methodology followed in this work was first intended to numerically solve Equations 1 and 2 using the finite volume method on a cylindrical geometry in order to obtain the temperature and concentration profiles in the fluid. Thereafter, Equations 3 and 4 were solved to obtain the mass fraction and the deposit thickness on the pipe surface.

A computer code in C++ language was developed to solve Equations 1 to 7, and the program flow chart is shown in Figure 2. The solution starts by introducing the physical properties of the oil and the operating conditions of the well subject to study.

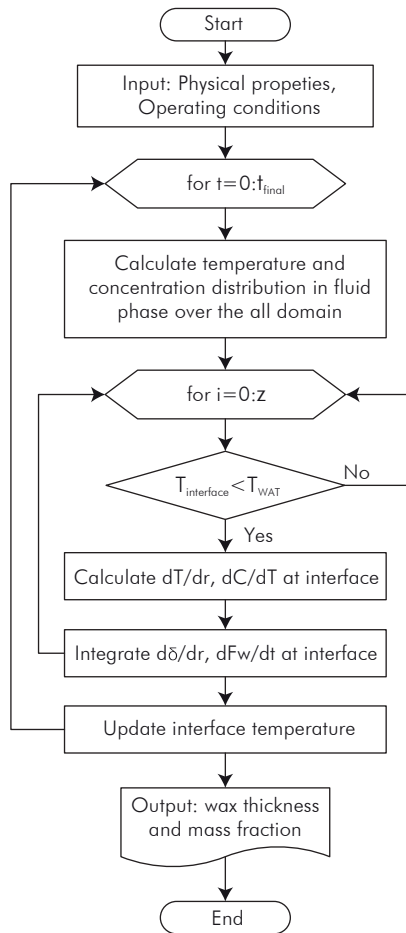


**Figure 2.** Program flow chart used to calculate wax thickness and mass fraction.

Then, in order to obtain the temperature and concentration profiles in the fluid phase energy (Equation 1) and mass (Equation 2) balances are solved accordingly. Afterwards, it is necessary to establish if the pipe wall temperature is lower than the WAT of the crude mixture. If this is the case, proceed to calculate the thermal and concentration gradients in this position. Thereafter, mass balances in the solid phase (Equation 3) and in the fluid-gel interface (Equation 7) are solved to obtain the thickness and paraffin fraction of the deposit. The procedure described above is repeated over all the axial domain of the pipe, namely, from  $L = 0$  to  $L = z$ .

Finally, this process is repeated for the desired time span previously chosen to evaluate the deposit, but not before updating the temperature in the fluid-gel interface since it increases as the deposit grows. Thus, the thickness profiles and paraffin fraction are obtained in the evaluated system.

### Validation

Once the solution was implemented, it was validated on the grounds of the experimental data published by Singh *et al.* (2000). They used a synthetic crude mixture made up by a mineral oil (Blandol) and Kerosene with a carbon number distribution between  $C_{23}$  and  $C_{38}$ . Physical properties and operating conditions used in the experimentation were reported by Singh *et al.* (2000) as shown in Table 2, while Figure 3 features the solubility curve.

**Table 2.** Physical properties and operating conditions used by Singh *et al.* (2000) during their experimentation.

Parameter	Value
Inner pipe radius	0.0072 (m)
Pipe length	2.44 (m)
Inlet temperature	22.2 (°C)
Wall temperature	7.2 (°C)
WAT	13.9 (°C)
Flow velocity	0.387 (m/s)
Density of wax	838.5 (kg/m <sup>3</sup> )
Density of oil	838.5 (kg/m <sup>3</sup> )
Heat capacity of oil	2259 (J/kg·K)
Thermal conductivity of oil	0.1466 (W/m·K)
Thermal conductivity of wax	0.25 (W/m·K)

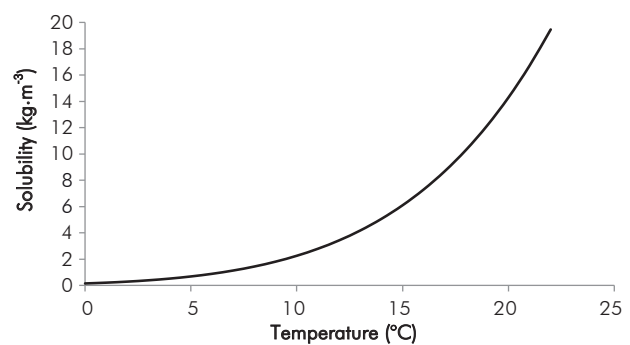


**Figure 3.** Solubility curve of the synthetic crude used by Singh *et al.* (2000) during their experimentation.

### Evaluation of Specific Boundary Conditions on Pipe Wall

Once the model was validated, it was applied to a specific production pipe considering three different

boundary conditions on the wall, one with a constant temperature and two considering a temperature profile. It is important to emphasize on the importance of the boundary condition as it has a significant influence on the deposition phenomenon depending on the location of the well. Three possible situations could promote the paraffin deposition: i) the experimental case studied by Singh *et al.* (2000) in which the wall temperature of the pipe remains constant and was used in this work to validate the model solution (Figure 4a); ii) the offshore production case in which the temperature of crude oil decreases as soon as it leaves the shore but then, it heats until reaching the surface temperature (Figure 4b) and iii) the common onshore case in which crude oil gets cold while raising to the surface due to the characteristic geothermal gradient of the environment where the production pipe is located (Figure 4c).

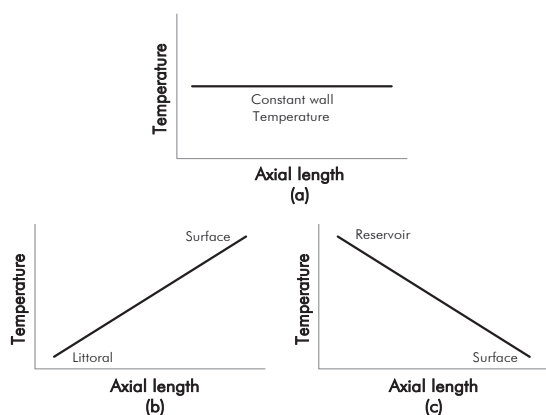


**Figure 4.** Axial thermal gradients during oil production (a) experimental case studied by Singh *et al.* (2000) under the following assumptions: a) a constant wall temperature; (b) wall boundary condition in case of offshore production (positive slope) and (c) common onshore production (negative slope).

Simulations were carried out considering three different flow rates,  $2.95 \times 10^{-5} \text{ m}^3 \cdot \text{s}^{-1}$  (V1),  $4.05 \times 10^{-5} \text{ m}^3 \cdot \text{s}^{-1}$  (V2) and  $5.28 \times 10^{-5} \text{ m}^3 \cdot \text{s}^{-1}$  (V3); and ten days of pipe operation in order to observe the effect of the aforementioned boundary conditions applied to the deposit thickness. Physical properties and operating conditions are summarized in Table 3 and were obtained from Ariza (2008), particularly, referring to paraffinic dead oil obtained from a Colombian oilfield (Colorado Field). Likewise, Figure 5 features the solubility curve of this oil, which was obtained from a Differential Scanning Calorimetry (DSC) test following the ASTM D4419-90 procedure. Subsequently, the thermogram obtained was

integrated assuming that the total energy released during the cooling or heating process is proportional to the area between the base line in the thermogram and the exothermal or endothermal peaks, respectively (Alcazar-Vara & Buenrostro-Gonzalez, 2013). According to the foregoing, it was found that the solubility limit of the paraffin in the crude mixture is  $29^\circ\text{C}$ .

**Table 3.** Physical properties and operating conditions used in the simulations.

Parameter	Value
Inner pipe radius	0.036(m)
Pipe length	1418.21(m)
Reservoir temperature	78.889 ( $^\circ\text{C}$ )
WAT	29 ( $^\circ\text{C}$ )
Oil density	797.2 ( $\text{kg}/\text{m}^3$ )
Oil heat capacity	2300 ( $\text{J}/\text{kg}\cdot\text{K}$ )
Oil thermal conductivity	0.1 ( $\text{W}/\text{m}\cdot\text{K}$ )
Paraffin thermal conductivity	0.25 ( $\text{W}/\text{m}\cdot\text{K}$ )

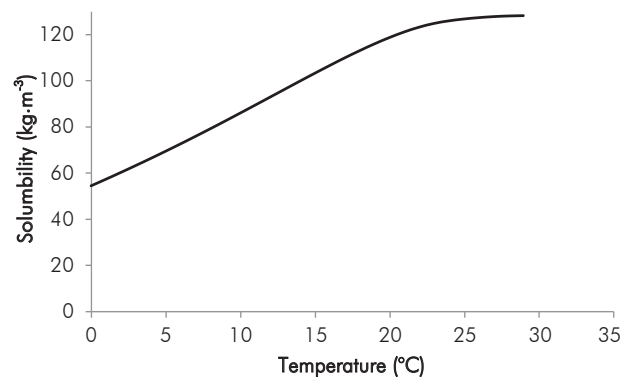


**Figure 5.** Solubility curve used in the simulations.

## 4. RESULTS AND DISCUSSION

### Validation

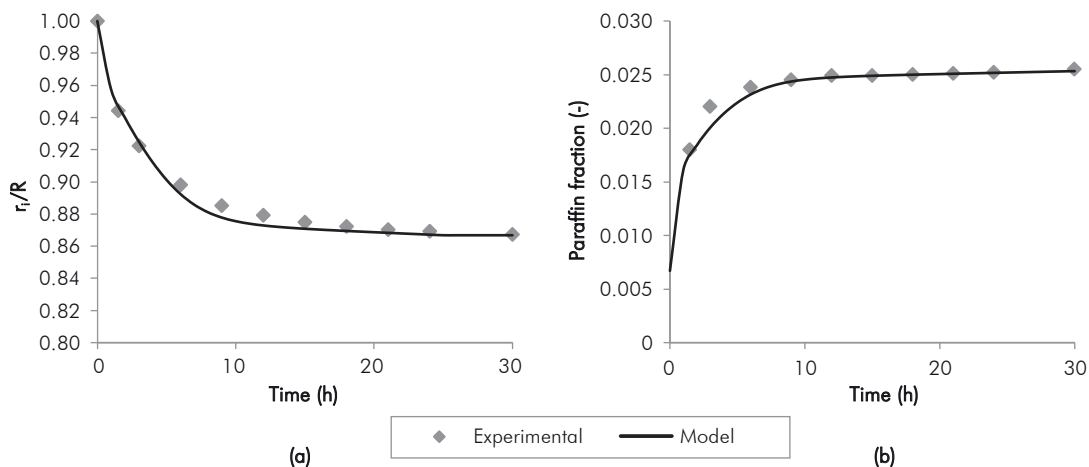
The numerical solution obtained in this work and the experimental results reported by Singh *et al.* (2000) were plotted in order for comparison purposes. Figures 6a and 6b show the radius change with regard to the inner pipe radius ( $r_i/R$ ) and the paraffin fraction inside the deposit as a function of time, respectively. The thickness change accounts for the way the pipe gets saturated with paraffin as a function of time; which shows the change of the

pipe radius due to the paraffin deposited on the wall as compared to the inner pipe radius.

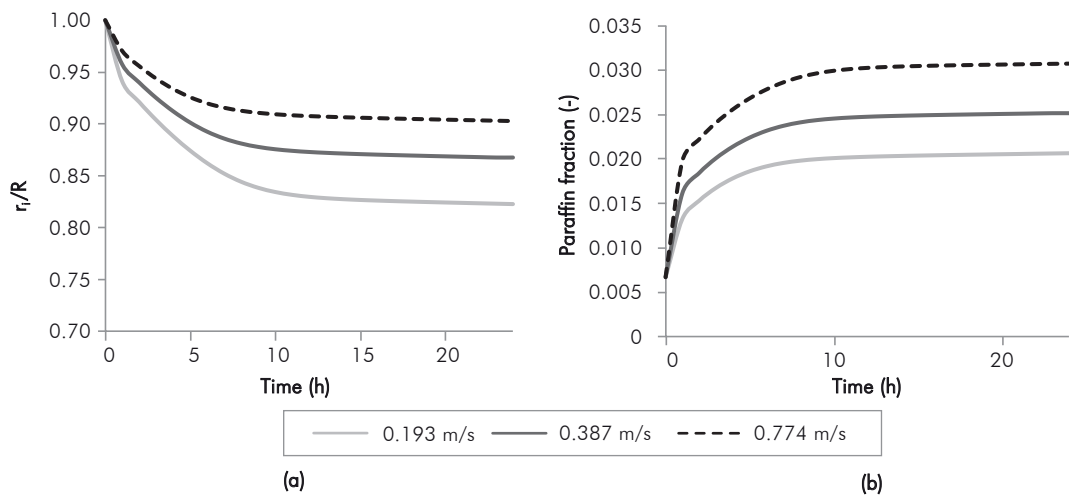
According to Figure 6a and 6b, there is a good match between both sets of results obtaining a maximum absolute error of 0.83% as for deposit thickness, while the paraffin fraction reached a maximum error of 2.8%. These low errors showed that the implemented model describes the paraffin deposition behavior in this system under the operating conditions described in the methodology. However, it was necessary to evaluate the behavior of these variables under other different operating conditions.

Figures 7a and 7b deal with the effect of the flow rate on the deposit thickness and paraffin fraction inside the deposit, respectively. According to these figures, it is possible to conclude that an increased flow rate causes a smaller deposit thickness but with higher paraffin concentration and, conversely; a decreased flow rate generates thicker deposits but with lower paraffin concentration. This can be explained by the effect of flow velocity that reduces the thermal gradient in radial direction when this is increased, and the concentration gradient at the same time.

Figure 8 shows the constant wall temperature ( $T_a$ ) effect on the paraffin deposit. According to this figure,

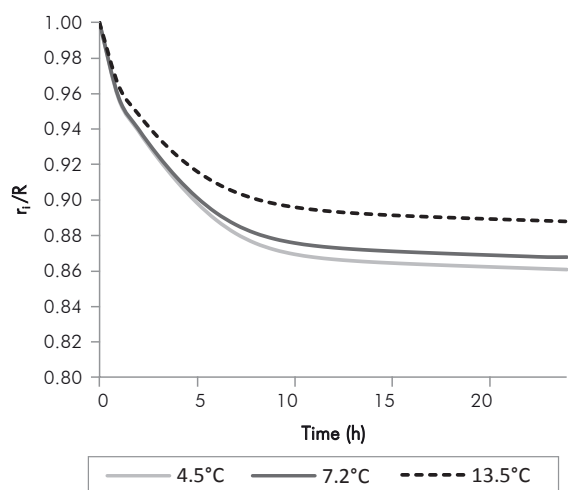


**Figure 6.** Comparison between the experimental results reported by Singh *et al.* (2000) and the implemented model (a) deposit thickness variation; (b) paraffin fraction.



**Figure 7.** Results obtained during the model implementation using data reported by Singh *et al.* (2000). (a) Flow rate effect on the deposit thickness; (b) Flow rate effect on the paraffin fraction.

when the wall temperature is reduced, the deposit thickness is increased and the opposite effect takes place when temperature is raised. This can be explained because when wall temperature is lower, the thermal gradient between the bulk and the wall is increased and at the same time, the concentration gradient increases as well, thus, promoting a higher mass transfer to the deposit.



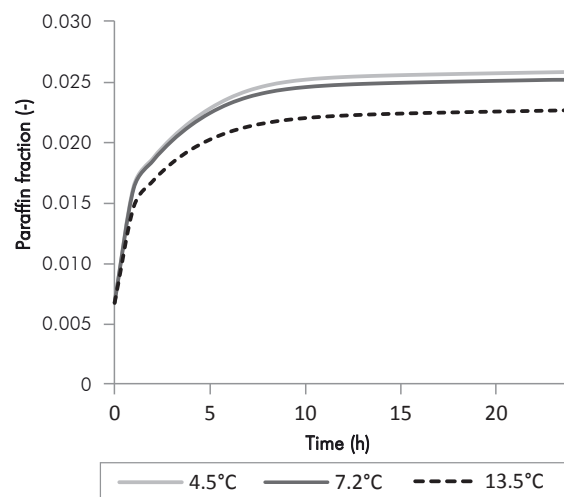
**Figure 8.** Wall temperature effect on the deposit thickness. Results obtained during the model implementation using data reported by Singh *et al.* (2000).

Figure 9 shows the wall temperature effect on the paraffin fraction inside the deposit for a constant wall temperature. It shows how paraffin fraction is increased when the wall temperature is reduced and the opposite effect when temperature is raised. This occurs because when the wall temperature is lower, the concentration gradient established between the bulk and the fluid-gel interface is increased, which enhance a higher paraffin transport inside the deposit.

The results shown above allow concluding that the model was successfully implemented under the conditions presented in the methodology and correspond to the results published by Singh *et al.* (2000).

### Application of the Model

Once the model was validated, it was implemented considering the three different boundary conditions described above. Figure 10 shows the deposit thickness along the pipe considering a constant wall temperature for a crude oil with physical properties shown in Table 3. This figure shows how maximum deposit thickness



**Figure 9.** Wall temperature effect on the paraffin fraction. Results obtained during the model implementation using data reported by Singh *et al.* (2000).

value is slightly reduced at the inlet of the pipe when the flow velocity is increased, however along the pipe it becomes evident that the deposit thickness tends to increase with an increased flow rate. A similar behavior is observed in Figure 11, which considers a wall temperature profile ascending as boundary condition on the pipe surface. A reduction in the maximum thickness value at the pipe inlet can be observed, together with an increase along the pipe as the flow rate increases. Nevertheless, in this case it is possible to observe how the deposit spreads over a short distance, approx. 200m after the inlet, point where the temperature of the fluid becomes higher than the WAT.

The dependence of the paraffin thickness on the flow rate can be explained, in the case of a constant wall temperature, from the results plotted in Figure 12, which shows the thermal gradient between the bulk and the wall versus the axial length of the pipe. According to this figure, it is clear that the temperature gradient (and hence the concentration gradient) tends rapidly to zero when the flow rate is lower; because the WAT is reached faster and therefore the deposit spreads over a shorter length. In contrast, an increased flow rate makes the WAT to be reached forward in the pipe and, consequently, the thermal gradient tends slowly to zero; promoting the deposit growth.

Moreover, analyzing Figure 13, which shows the thermal gradient in radial direction versus the axial

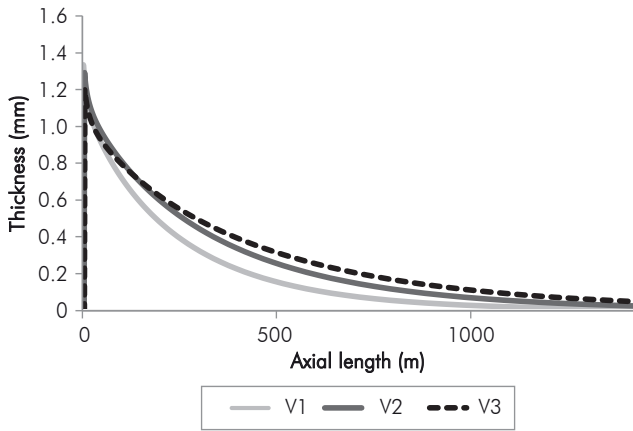


Figure 10. Deposit thickness considering a constant wall temperature at three different flow rates.

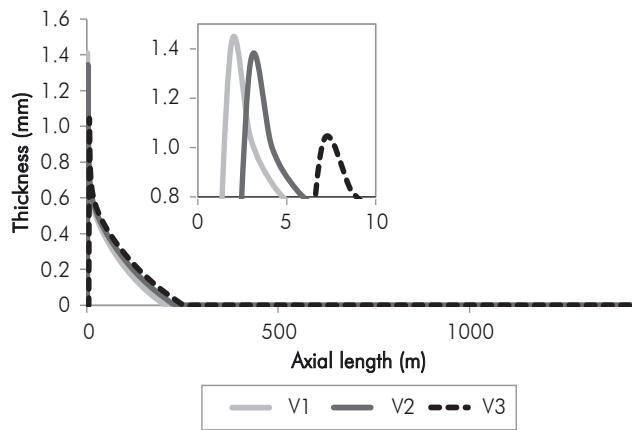


Figure 11. Deposit thickness considering an axial temperature gradient with a positive slope at three different flow rates.

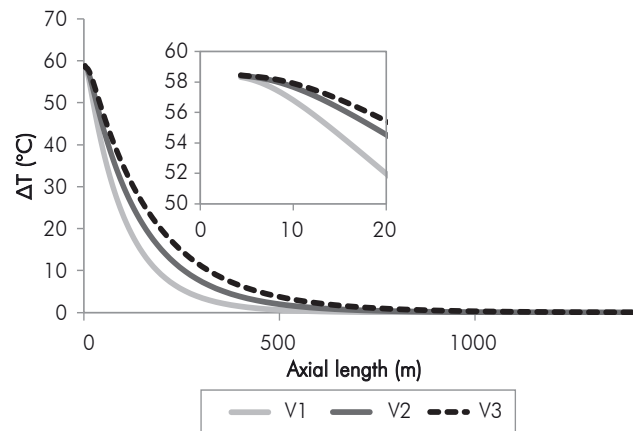


Figure 12. Temperature difference between the bulk and the wall considering a constant wall temperature at three different flow rates.

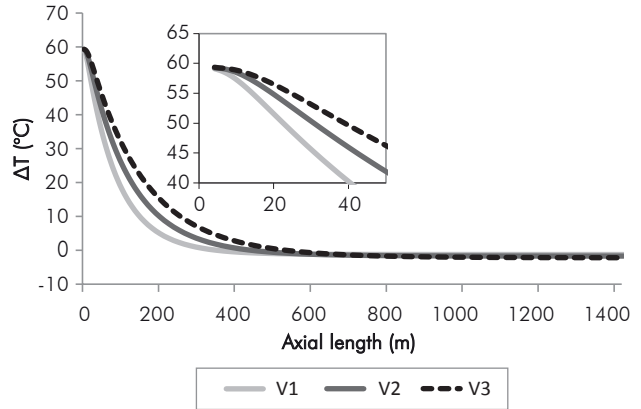


Figure 13. Temperature difference between the bulk and the wall considering an axial temperature gradient with a positive slope at three different flow rates.

distance of the pipe, it becomes clear that the negative gradient indicates that the crude oil starts flowing at a lower temperature than the WAT of the crude mixture, which allows for the deposit build-up. Nonetheless, while the fluid is flowing, the deposit temperature increase forced by the boundary condition applied to the wall, thus the fluid will reach the WAT first and later the wall temperature, in a shorter or longer distance depending on the flow rate. It means that if the flow rate is low, the crude will reach the wall temperature in a shorter section of the pipe, as opposite to high flow rates. However, if the crude oil reaches the WAT, the deposition process will stop regardless the thermal gradient remains.

Similarly, Figure 14 shows the deposit thickness versus axial distance when considering an axial thermal gradient with a negative slope for three different flow rates. It becomes evident that the maximum deposit thickness increases as the flow rate increases too. This differs from the cases above, where the wall temperature is constant or when an axial thermal gradient with a positive slope is considered. This can be explained because the order of magnitude of the convective term in the energy balance is kept constant while the radial diffusive term is reduced substantially due to the temperature gradient at the inlet of the pipe is approx. 20°C lower than the two cases previously presented (cf. Figure 15).

Finally, Figure 16 summarizes the plots of deposit thickness versus the axial distance, for the three boundary

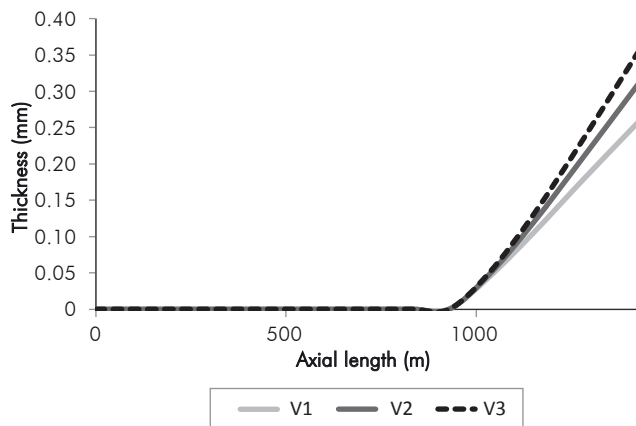


Figure 14. Deposit thickness considering an axial temperature gradient with a negative slope at three different flow rates.

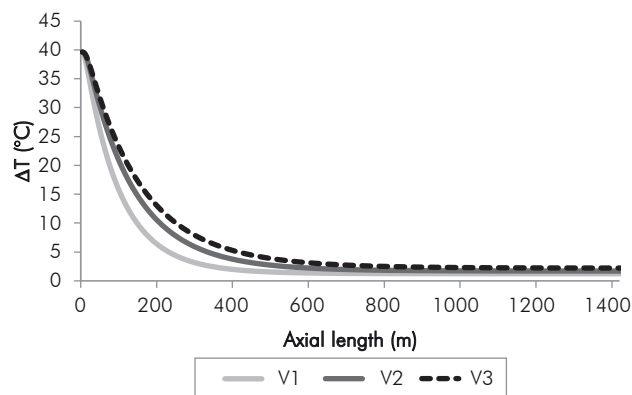


Figure 15. Temperature difference between the bulk and the wall considering an axial temperature gradient with a negative slope at three different flow rates.

conditions cases presented above, considering the same flow rate. This figure shows how under a constant wall temperature and a positive slope in the axial thermal gradient, the two deposit thickness curves have a similar shape, which means thickness is reduced from entrance to exit, but it spreads over a longer distance when the wall temperature is constant. However, when considering a negative slope in the axial thermal gradient; the deposit grows much further than the inlet of the pipe, and the maximum thickness is lower than the other cases, which means this case is less severe. This could be explained by noting the maximum thermal gradient, which is approximately 20°C lower than other two cases, which translates also into a lower concentration gradient and hence a lower paraffin flow inside the deposit.

Moreover, it worth mentioning that it is not possible to compare the thickness obtained when the wall

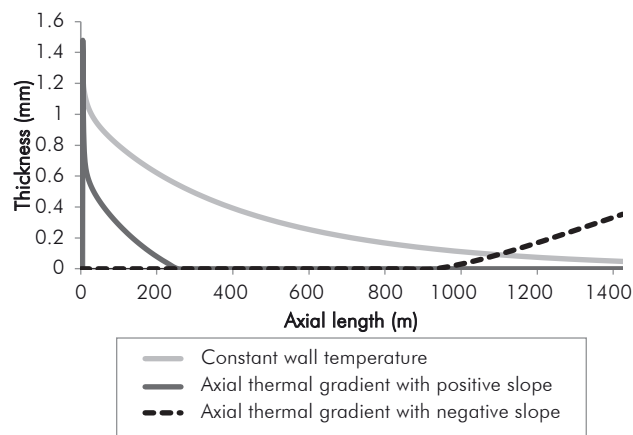


Figure 16. Three different boundary conditions studied.

temperature is constant with the other cases where a temperature profile was considered, because the deposit thickness will depend on how far is the wall temperature from the WAT. Nevertheless, when an axial temperature profile was considered, the same gradient (20°C) was assured in order to compare each other. Therefore, the maximum thickness was reached when an axial thermal gradient with a positive slope was considered as shown in Figure 16. This is due to the dramatic change of temperature experienced by the fluid at the inlet of the pipe, and the oil mixture immediately reaches the solubility limit; which causes a greater radial thermal gradient and consequently a higher thickness. While in the case of a negative slope, the temperature change is not so dramatic but it does increase when the temperature gradients have been reduced already.

However, by comparing deposit sizes, not the maximum thickness, following the integration of each plot, it was found that axial thermal gradients with a negative slope are slightly bigger (approx. 1.2 times) than in the other case as shown in Figure 16. Thus, even though there is more paraffin deposition with the negative slope, the deposit is thicker in the positive slope case, which is more harmful for the pipe.

## 5. CONCLUSION

This work implements the wax deposition model proposed by Singh *et al.* (2000) and applied to a paraffinic crude. It was found that when considering a temperature profile in the pipe wall, the maximum paraffin deposit thickness is increased or reduced depending on

whether the profile has a positive or a negative slope, respectively, particularly, when compared to a constant pipe wall temperature. The effect of operating conditions such as flow rate; deposition time and wall temperature of the pipe was evaluated over the deposit thickness. The results showed that an increased flow rate reduces the maximum deposit thickness but it spreads over a longer distance in the pipe when considering a constant wall temperature or an axial thermal gradient with a positive slope. Moreover, a comparison of both cases of axial thermal gradients was used to find out that a thicker paraffin deposit is reached when the gradient has a positive slope instead a negative one; but when considering all the mass deposited on the pipe wall, it was found that the case of the thermal gradient with a negative slope is bigger than the other. However, it is more harmful for the pipe to have a thicker deposit rather than having one spread over a longer distance in the pipe, but thinner. Finally, the implementation of the Singh *et al.* (2000) model, or more complex ones, could be useful to forecast the paraffin deposition severity, as well as in the implementation of preventive techniques.

## ACKNOWLEDGEMENTS

Authors want to thank the Office for Research and Extension of *Universidad Industrial de Santander* for supporting the research, by the global project named “*Desarrollo de una herramienta computacional para la simulación del flujo multifásico de pozos petroleros del Campo Escuela Colorado*”.

## REFERENCES

- Alcazar-Vara, L. A. & Buenrostro-Gonzalez, E. (2013). Liquid-solid phase equilibria of paraffinic systems by DSC measurements. In: Elkordy, A. A. *Applications of calorimetry in a wide context - Differential Scanning Calorimetry, isothermal titration calorimetry and microcalorimetry*. Rijeka: InTech. Chapter 11, 253-276.
- Ariza, E. (2008). Determinación del umbral de cristalización de las parafinas en el crudo del Campo Colorado. *Tesis de Maestría, Ingeniería de Petróleos*, Universidad Industrial de Santander, Bucaramanga, Colombia, 93pp.
- ASTM Standard D4419-90. Standard Test Method for Measurement of Transition Temperatures of Petroleum Waxes by Differential Scanning Calorimetry (DSC). *Annual Book of ASTM Standards*, Vol. 05.02, ASTM International, West Conshohocken, PA, 2010.
- Burger, E., Perkins, T. & Striegler, J. (1981). Studies of wax deposition in the Trans Alaska pipeline. *J. Petrol. Technol.*, 33(6), 1075-1086.
- Coutinho, J. A. P., & Daridon, J. L. (2001). Low pressure modeling of wax formation in crude oils. *Energy Fuels*, 15(6), 1454-1460.
- Coutinho, J. A. P., Mirante, F. & Pauly, J. (2006). A new predictive UNIQUAC for modeling of wax formation in hydrocarbon fluids. *Fluid Phase Equilib.*, 247(1-2), 8-17.
- Cussler, E. L., Hughes, S. E., Ward, W. J. & Aris, R. (1998). Barrier membranes. *J. Membrane Sci.*, 38(2), 161-174.
- Gjermundsen, I. (2006). State of the art: Wax precipitation deposition and aging in flowing hydrocarbon systems. *Internal Report*, Norsk Hydro ASA, Porsgrunn, Norway.
- Hayduk, W. & Minhas, B. S. (1982). Correlations for prediction of molecular diffusivities in liquids. *Can. J. Chem. Eng.*, 60(2), 295-299.
- Hovden, L., Rønningsen, H. P., Xu, Z. G., Labes-Carrier, C. & Rydahl, A. (2004). Pipeline wax deposition models and model for removal of wax by pigging: Comparison between model predictions and operational experience. *4th North American Conference on Multiphase Technology*, Banff, Canada.
- Huang, Z., Lee, H. S., Senra, M. & Fogler, H. S. (2011). A fundamental model of wax deposition in subsea oil pipelines. *AIChE J.*, 57(11), 2955-2964.
- Lee H. S. (2007). Computational and rheological study of wax deposition and gelation in subsea pipelines. *Ph.D Thesis, Chemical Engineering*, University of Michigan, USA, 127 pp.
- Lu, Y., Huang, Z., Hoffmann, R., Amundsen, L. & Fogler, H. S. (2012). Counterintuitive effects of the oil flow rate on wax deposition. *Energy Fuels*, 26(7), 4091-4097.
- Matzain, A., Apte, M. S., Zhang, H., Volk, M., Redus, C. L., Brill, J. P. & Creek, J. L. (2001). Multiphase flow wax deposition modeling. *Proceedings Engineering Technology Conference on Energy*. Houston, USA, ETCE 17114.
- Rygg, O. B., Rydahl, A. K. & Rønningsen, H. P. (1998). Wax deposition in offshore pipeline systems. *Proc. 1st North American Conference on Multiphase Technology*, Banff, Canada.

Singh, P., Venkatesan, R., Fogler, H. S. & Nagarajan, N. (2000). Formation and aging of incipient thin film wax-oil gels. *AIChE J.*, 46(5), 1059-1074.

Svendsen, J. A. (1993). Mathematical modeling of wax deposition in oil pipeline systems, *AIChE J.*, 39(8), 1377-1388.

Tian, Z., Jin, W., Wang, L. & Jin, Z. (2014). The study of temperature profile inside wax deposition layer of waxy crude oil in pipeline. *FHMT*, 5(5), 1-8.

---

## AUTHORS

### **Diego-Fernando Bautista-Parada**

Affiliation: *Universidad Industrial de Santander*

Chemical Engineering, *Universidad Industrial de Santander*

M. Sc. in Chemical Engineering, *Universidad Industrial de Santander*

e-mail: diegof\_7@hotmail.com

### **David-Alfredo Fuentes-Díaz**

Affiliation: *Universidad Industrial de Santander*

Mechanical Engineering, *Universidad Industrial de Santander*

Ph. D. in Energy Technology, *Universidad Politécnica de Valencia*

e-mail: dfuentes@uis.edu.co

### **Paola Gauthier-Maradei**

Affiliation: *Universidad Industrial de Santander*

Chemical Engineering, *Universidad Industrial de Santander*

M. Sc. in Chimie Appliquée et Génie des Procédés Industriels, *Université Pierre et Marie Curie*

Ph. D. in Chemistry, *Institut Français du Pétrole*

e-mail: mapaomar@uis.edu.co

### **Arlex Chaves-Guerrero**

Affiliation: *Universidad Industrial de Santander*

Chemical Engineering, *Universidad del Valle*

Spe. in Thermal Sciences, *Universidad del Valle*

M. Sc. in Mechanical Engineering, *Universidad de Puerto Rico*

Ph. D. in Chemical Engineering, *Universidad de Puerto Rico*

e-mail: achavesg@uis.edu.co

**NOTATION**

$C$	Mass concentration
$C_{wb}$	Bulk concentration of paraffin
$C_{ws}$	Paraffin solubility in the oil
$D_e$	Effective diffusivity in the deposit
$D_{wo}$	Paraffin diffusivity in the oil
$F_w$	Mass fraction of the gel
$k_l$	Mass transfer coefficient
$L$	Length of the pipe
$R$	Inner radius
$r$	Radial coordinate
$r_i$	Deposit position
$T$	Temperature
$V_A$	Molar volume of the paraffin
$v_z$	Axial velocity
$z$	Axial coordinate

**GREEK SYMBOLS**

$\alpha$	Aspect ratio of the wax crystals in the deposit
$\alpha_T$	Thermal diffusivity
$\mu$	Solvent viscosity
$\rho_{gel}$	Wax density